



Conjugate natural convection heat transfer in a planar thermosyphon with multiple inlets
by John Joseph Fleming

A thesis submitted in partial fulfillment of the requirements for the degree of Master of Science in
Mechanical Engineering
Montana State University
© Copyright by John Joseph Fleming (1994)

Abstract:

The heat transfer results for the numerical investigation of a planar open loop thermosyphon are presented. The thermosyphon flow path is a modified "U" shape. Laminar flow is by natural convection due to heating the left ascending channel of the "U". Air ($Pr=0.71$) enters at the top and bottom of the right descending channel. The center portion of the "U" is a solid conducting wall and the left channel is bounded by a conducting wall. The left wall is heated isothermally along its external surface. All other external surfaces are adiabatic. This configuration is a modification of heat removal systems used in passive reactor cooling, nuclear waste material storage, and various other applications.

The average Nusselt number for this configuration was studied for different values of the governing parameters. These include the Rayleigh number, the ascending channel aspect ratio, the lower inlet width, and the wall thermal conductivity. These results are obtained using the proprietary finite element analysis program COSMOS/M to numerically solve the governing equations.

The average Nusselt number (Nu) is strongly affected by the wall thermal conductivity primarily due to conduction resistance of the heated wall. For restrictive lower inlet widths and low Rayleigh numbers (Ra), Nu decreases. At large Ra however, Nu depends little on the lower inlet width. This is due to compensating inflow at the outlet (recirculation). Recirculation is due to inlet flow restrictions and a developing thermal boundary layer at the heated wall which allows cool reservoir fluid access via the outlet. It is shown that Nu depends on the ascending channel aspect ratio. Another parameter which combines the heated wall geometry and thermal conductivity into one parameter is demonstrated to correlate the heat transfer results well.

The results are compared to published experimental results for a similar problem. The comparison indicates that the present thermosyphon configuration is an efficient heat transfer device for sufficiently large wall , thermal conductivity and lower values of Ra .

CONJUGATE NATURAL CONVECTION HEAT TRANSFER IN A
PLANAR THERMOSYPHON WITH MULTIPLE INLETS

by

John Joseph Fleming

A thesis submitted in partial fulfillment of the
requirements for the degree

of

Master of Science

in

Mechanical Engineering

MONTANA STATE UNIVERSITY
Bozeman, Montana

April 1994

0

71378
F629

APPROVAL

of a thesis submitted by

John Joseph Fleming

This thesis has been read by each member of the thesis committee and has been found to be satisfactory regarding content, English usage, format, citations, bibliographic style, and consistency, and is ready for submission to the College of Graduate Studies.

18 April 1994

Date

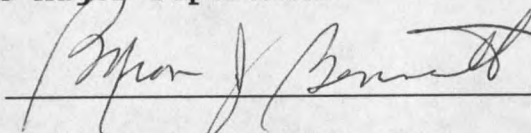


Chairperson, Graduate Committee

Approved for the Major Department

18 April 1994

Date



Head, Major Department

Approved for the College of Graduate Studies

4/26/94

Date



Graduate Dean

STATEMENT OF PERMISSION TO USE

In presenting this thesis in partial fulfillment of the requirements for a Master's degree at Montana State University, I agree that the Library shall make it available to borrowers under the rules of the Library.

If I have indicated my intention to copyright this thesis by including a copyright notice page, copying is allowable only for scholarly purposes, consistent with "fair use" as prescribed in the U. S. Copyright Law. Requests for permission for extended quotation from or reproduction of this thesis in whole or in parts may be granted only by the copyright holder.

Signature

John S. J. [Signature]

Date

4/19/94

ACKNOWLEDGEMENTS

I would like to thank Dr. Ruhul Amin for his guidance in the development of this project. I would like to express my appreciation to Dr. Alan George and Dr. Thomas Reihman for their work as committee members.

I would also like to thank Dr. Randy Clarksean at Argonne National Laboratory Idaho Falls for his valuable comments to Dr. Amin during the initial stage of this project.

My deepest appreciation is extended to my wife, Janice, for her understanding and endurance, and to John Gable for his support.

TABLE OF CONTENTS

	<u>Page</u>
LIST OF TABLES	vi
LIST OF FIGURES	vii
NOMENCLATURE	ix
ABSTRACT	xii
INTRODUCTION	1
Motivation for Present Research	4
Problem Description	5
Background	9
PROBLEM FORMULATION	16
Introduction	16
Governing Equations	16
Normalization of Governing Equations	22
NUMERICAL INVESTIGATION	31
Introduction	31
Computational Matrix	31
Computational Mesh	37
RESULTS AND DISCUSSION	42
Introduction	42
Effect of Lower Inlet Width Parameter	46
Effect of Thermal Conductivity Parameter	65
Average Nusselt Number Dependencies	79
Wall Conductivity Parameter	90
Aspect Ratio Parameter	93
CONCLUSIONS AND RECOMMENDATIONS	95
REFERENCES	98
APPENDICES	102
Appendix A-COSMOS/M Finite Element Program	103
Appendix B-FORTRAN Programs	110
Program to Compute Internal Average Nusselt Number	111
Program to Compute External Average Nusselt Number	114
Program for Combining COSMOS/M Output Files	116

LIST OF TABLES

<u>Table</u>	<u>Page</u>
1. Parameter values and ranges of interest	33
2. Computational matrix with fixed aspect ratio Ar = 6	35
3. Computational matrix with fixed aspect ratio Ar = 3	36
4. Results of mesh independence tests	39
5. Computed average Nusselt numbers for the benchmark solution vs. the COSMOS/M solution	40
6. Heated wall conductivity study parameter	90
7. Overall Nusselt number results for K_r study	91
9. Aspect ratio study parameters	93

LIST OF FIGURES

<u>Figure</u>	<u>Page</u>
1. General open loop thermosyphon configuration . . .	2
2. Schematic diagram of problem geometry	6
3. Schematic diagram of problem showing boundary conditions	21
4. Basic geometric configurations	34
5. Element distribution meshes "B" and "A" ($W_2=0.75$)	41
6. Isotherm plots with $K=5$ and $Ar=6$ for varying W_2 and Ra	48
7. Stream function plots with $K=5$ and $Ar=6$ for varying W_2 and Ra	50
8. Total mass inflow rate from all sources vs. Ra .	54
9. Total mass inflow rate from lower and upper inlets vs. Ra	54
10. Temperature distribution across outlet with parameters W_2 and Ra	57
11. Vertical velocity distribution across outlet with parameters W_2 and Ra	58
12. Heat transfer to upper inlet as a percent of total heat transfer ($(Q_p/Q_w)100$) vs. Ra	60
13. Ratio of upper inlet to lower inlet mass flow rate (M_u/M_l) vs. Ra	60
14. Heated wall and fluid interface local Nusselt number distribution with parameters W_2 and Ra	62
15. Heated wall and fluid interface temperature distribution with parameters W_2 and Ra	63
16. Isotherm plots with $W_2=0.25$ and $Ar=6$ for varying K and Ra	67
17. Stream function plots with $W_2=0.25$ and $Ar=6$ for varying K and Ra	69

LIST OF FIGURES-continued

18.	Heated wall and fluid interface temperature distribution with parameters K and Ra	72
19.	Vertical velocity distribution across outlet with parameters K and Ra	75
20.	Temperature distribution across outlet with parameters K and Ra	76
21.	Heat transfer to upper inlet as a percent of total heat transfer $((Q_p/Q_w)100)$ vs. Ra	77
22.	Ratio of upper inlet to lower inlet mass flow rate (M_u/M_l) vs. Ra	77
23.	Total mass inflow rate from all sources vs. Ra .	78
24.	Total mass inflow rate from lower and upper inlets vs. Ra	78
25.	Average Nusselt number vs. Rayleigh number with parameters W_2 and K	82
26.	Average Nusselt number vs. Rayleigh number with parameters K and W_2	84
27.	Published heat transfer results compared with Nu for the present problem	87
28.	Published heat transfer results compared with Nu_l for the present problem	89
29.	Constant K_x solid/fluid interface temperature distribution comparison cases 1 and 2	92
30.	Constant K_x solid/fluid interface local convection coefficient comparison cases 1 and 2	92
31.	Correlation of Nu results vs. the modified Rayleigh number with constant K_x	94
32.	Program to compute internal average Nusselt number	111
33.	Program to compute external average Nusselt number	114
34.	Program for combining COSMOS/M output files . .	116

NOMENCLATURE

<u>Symbol</u>	<u>Description</u>
Ar	inner channel aspect ratio, l_1/b
b	inner channel width
B	nondimensional inner channel width b/b
C_p	constant pressure specific heat
g_y	acceleration due to gravity
\vec{g}	acceleration vector
Gr	Grashof number $g_y \beta (T_w - T_\infty) b^3 / \nu^2$
h_1	left wall thickness
H_1	nondimensional left wall thickness h_1/b
h_2	partition wall thickness
H_2	nondimensional partition wall thickness h_2/b
k	thermal conductivity
K	thermal conductivity ratio k_w/k_a
K_r	wall conductivity parameter $K_r = k_w l_1 / k_a h_1 = K(L_1/H_1)$
l_1	inner channel height
L_1	nondimensional inner channel height l_1/b
l_2	lower inlet length
L_2	nondimensional lower inlet length l_2/b
M	nondimensional mass flow rate $M = \dot{m} / \mu b$
Nu	average Nusselt number $Nu = \bar{q} b / k_a (T_w - T_\infty)$
Nu_1	average Nusselt number (equation 54)
p	pressure

NOMENCLATURE-continued

p_h	hydrostatic pressure
p_m	motion pressure ($p - p_h$)
Pr	Prandtl number ν/α
\bar{q}	average local heat flux
Q_p	total heat transfer across partition wall
Q_w	total heat transfer across heated wall
Ra	Rayleigh number $g_y \beta (T_w - T_\infty) b^3 / \alpha \nu$
T	temperature
T_o	reference temperature
\vec{u}	velocity vector
U_o	characteristic velocity
u	horizontal velocity
v	vertical velocity
w_1	upper inlet width
W_1	nondimensional upper inlet width w_1/b
w_2	lower inlet width
W_2	nondimensional lower inlet width w_2/b
x	cartesian x coordinate
y	cartesian y coordinate

Greek Symbols

α	thermal diffusivity
β	coefficient of volumetric expansion
θ	nondimensional temperature $(T - T_\infty) / (T_w - T_\infty)$

NOMENCLATURE-continued

μ	dynamic viscosity
ν	kinematic viscosity
ρ	density
τ_{xx}, τ_{yy}	normal stresses
ψ	stream function
ψ^*	nondimensional stream function $\psi^* = \psi/\nu$

Subscripts and Superscripts

a	working fluid (air) value
i	solid/fluid interface value
l	lower inlet value
p	partition value
m	maximum
n	direction normal to surface
p	partition value
r	right wall value
u	upper inlet value
w	heated wall value
∞	ambient value
*	nondimensional quantity

ABSTRACT

The heat transfer results for the numerical investigation of a planar open loop thermosyphon are presented. The thermosyphon flow path is a modified "U" shape. Laminar flow is by natural convection due to heating the left ascending channel of the "U". Air ($Pr=0.71$) enters at the top and bottom of the right descending channel. The center portion of the "U" is a solid conducting wall and the left channel is bounded by a conducting wall. The left wall is heated isothermally along its external surface. All other external surfaces are adiabatic. This configuration is a modification of heat removal systems used in passive reactor cooling, nuclear waste material storage, and various other applications.

The average Nusselt number for this configuration was studied for different values of the governing parameters. These include the Rayleigh number, the ascending channel aspect ratio, the lower inlet width, and the wall thermal conductivity. These results are obtained using the proprietary finite element analysis program COSMOS/M to numerically solve the governing equations.

The average Nusselt number (Nu) is strongly affected by the wall thermal conductivity primarily due to conduction resistance of the heated wall. For restrictive lower inlet widths and low Rayleigh numbers (Ra), Nu decreases. At large Ra however, Nu depends little on the lower inlet width. This is due to compensating inflow at the outlet (recirculation). Recirculation is due to inlet flow restrictions and a developing thermal boundary layer at the heated wall which allows cool reservoir fluid access via the outlet. It is shown that Nu depends on the ascending channel aspect ratio. Another parameter which combines the heated wall geometry and thermal conductivity into one parameter is demonstrated to correlate the heat transfer results well.

The results are compared to published experimental results for a similar problem. The comparison indicates that the present thermosyphon configuration is an efficient heat transfer device for sufficiently large wall thermal conductivity and lower values of Ra .

INTRODUCTION

Natural convection heat transfer has been an area of increasing interest for many years. This interest is prompted by the wide variety of useful engineering applications in which natural convection is an important (or dominant) mode of heat transfer. Natural convection results from buoyancy forces which arise from the interaction of density variations within a fluid and a body force, usually gravity. The density variation is often due to temperature gradients in which case the flow is driven by thermal buoyancy forces. Natural convection is inherently reliable because it is completely self-sustaining; it requires no external pumps as does forced convection to initiate and maintain fluid circulation. This also makes it a relatively low cost heat transfer method, both for initial setup and for operation and maintenance.

Natural convection flows are governed by the conservation laws for mass, momentum, and energy. These laws expressed in mathematical form become a system of coupled, nonlinear partial differential equations. For all non-isothermal buoyancy induced flows the temperature and velocity fields are coupled and must be solved simultaneously.

Analytical solutions for natural convection flows exist for a relatively few situations. Most complex flows of engineering interest are not open to analytical methods, so numerical and experimental methods are relied upon. The

present study is strictly a numerical investigation. It should be noted that numerical results can only be validated by experiment.

The thermosyphon is a natural convection heat transfer device or configuration which makes use of thermal buoyancy forces to drive fluid circulation in systems that may be closed, partially open, or fully open. Of interest here is the open loop thermosyphon in which a circulating fluid is exchanged with a large external (nearly) constant temperature reservoir. The schematic of a typical configuration forming a "U" shaped flow path is shown in Figure 1.

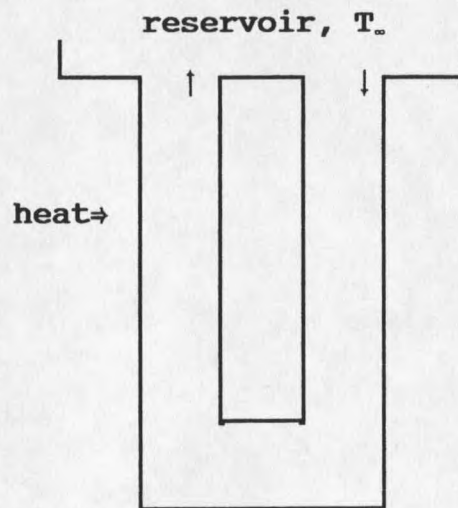


Figure 1. General open loop thermosyphon configuration.

Heat energy is transferred to the fluid in the left ascending leg of the thermosyphon. This causes the fluid to flow upwards due to the thermal buoyancy force. The flow in the ascending leg draws reservoir fluid into the right

descending leg establishing a continuous "open" flow loop.

Open loop thermosyphons have been successfully applied in a number of engineering applications. Cooling of electronic components is an important application [Jaluria (1985)]. Solar energy collection systems utilize natural convection extensively [Kreith and Anderson (1985)]. As shown by Clarksean (1993), passive heat removal from stored nuclear materials is an area of recent interest. Cooling of gas turbine blades is another important application [Japikse (1973)]. On a much larger scale, geothermal processes have been modelled as open loop thermosyphons [Torrance (1979)]. The following provides more detail of an important application of current interest.

The U. S. advanced liquid metal reactor (ALMR) design utilizes an open loop thermosyphon configuration to achieve inherently safe heat removal from a nuclear reactor in the event of the loss of primary coolant [Kwant and Boardman, (1992)]. This passive cooling system known as the reactor vessel auxiliary cooling system (RVAC) can be conceptually described as three vertical concentric cylinders: an inner, an intermediate, and an outer cylinder closed at the bottom. The inner cylinder is the reactor where heat is generated. Air heated by the hot reactor surface flows upward due to thermal buoyancy forces. This flow draws atmospheric air down an outer channel formed by the outer and intermediate cylinders. The resulting steady flow cools the reactor passively and

automatically. The system is designed so that in the event of primary coolant loss, safe reactor temperature levels will not be exceeded. The RVAC system is an important part of the power reactor inherently safe module (PRISM) design strategy.

Motivation for Present Research

Given the inherent reliability and importance of the open loop thermosyphon described above, further understanding is desirable in order to predict performance and optimize design parameters. A literature survey found many studies on natural convection between vertical parallel plates (a form of open loop thermosyphon) with a variety of boundary conditions. Also, some research has been conducted on the general "U" type geometry as in the RVAC system. Few studies however, have explicitly taken into account the thickness and finite thermal conductivity of the bounding wall surfaces. Research of natural convection in enclosures and vertical channels has indicated that the wall material and geometry were often significant parameters.

Previous research investigated open loop thermosyphons with the general "U" type flow configuration (one inlet and outlet) as shown in Figure 1. Modified open loop geometries with more than one inlet have not been explored. Further, no literature was found on the combined effect of wall conductivity and configuration of multiple flow inlets.

Greater understanding of these parameters is required for the optimization of open loop thermosyphons in engineering applications.

Problem Description

The objective of the present study is to conduct a steady state numerical investigation of the heat transfer characteristics of a single phase open loop thermosyphon. The geometry of the problem considered here is shown in Figure 2.

Linear dimensions in Figure 2 are shown in lower case, while the corresponding normalized dimensions are in upper case and enclosed in parentheses. All linear dimensions are normalized with respect to the inner channel width ($B=1$).

A Newtonian fluid (air, $Pr=0.71$) flows in the planar thermosyphon and is exchanged with constant temperature (T_∞) surroundings. A partition wall, a left wall, and a right wall of the same material, form the outer and inner channels. Fluid may enter the thermosyphon at two inlets placed at the upper and lower extremities of the outer channel. Fluid exits to the surroundings from the top of the inner left channel.

The flow is driven by a constant temperature boundary condition (T_w) applied at the left wall external surface. All other external surfaces are considered adiabatic. The computational domain is restricted to the thermosyphon to reduce computation time required. Thus, boundary conditions at the flow inlets and outlet are important considerations.

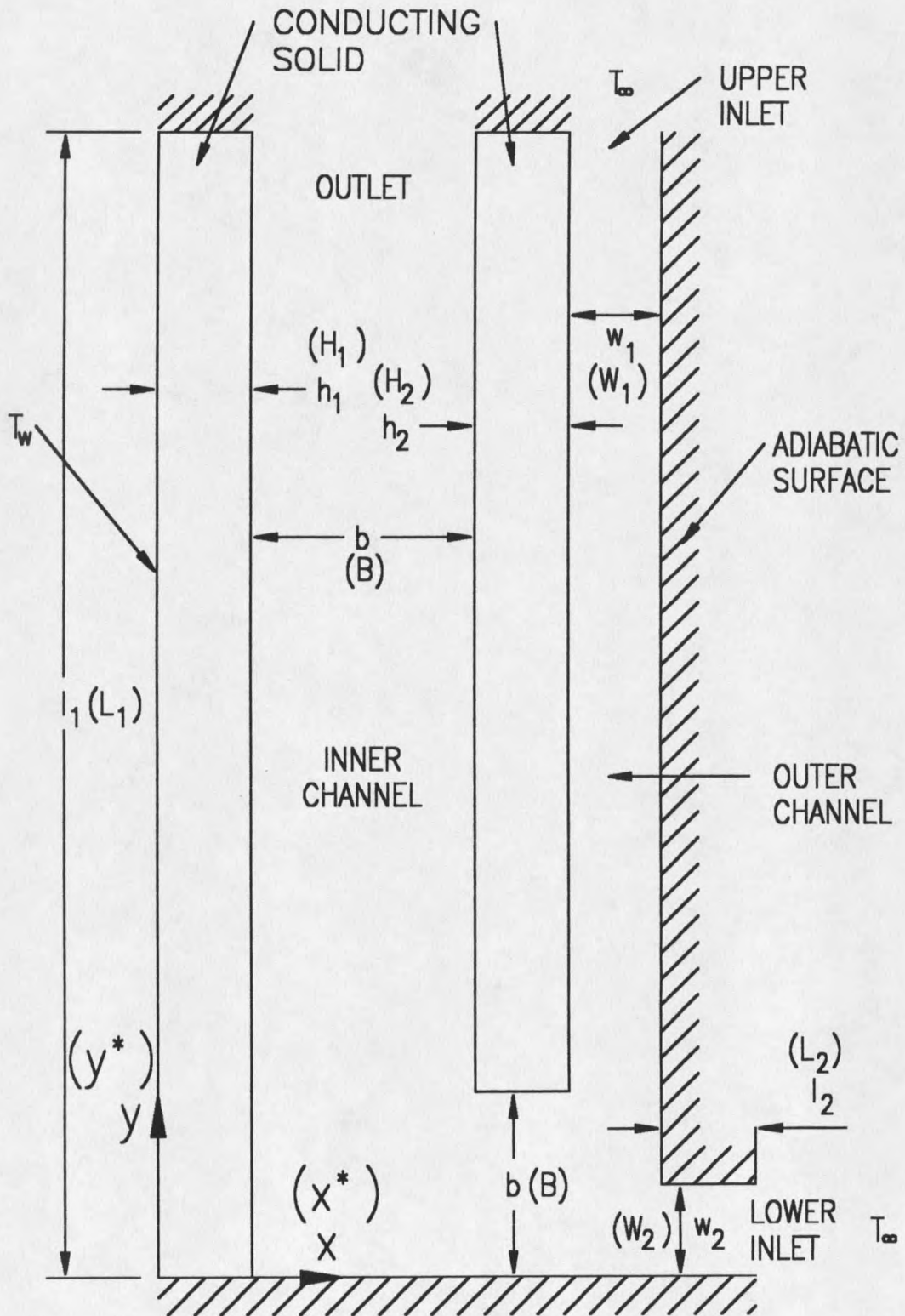


Figure 2. Schematic diagram of problem geometry.

Fluid enters the thermosyphon at the temperature of the surroundings (T_∞). The exiting fluid temperature is part of the solution and is not known a priori. A temperature boundary condition must be applied at the exit, so an approximate condition is specified. Previous work [Abib and Jaluria (1988)] has shown that setting the temperature gradient equal to zero in the vertical direction at the exit adequately approximates the interaction between the surroundings and the thermosyphon. Lateral fluid velocity and normal stress are also set equal to zero to complete the boundary conditions at the inlets and outlet. The Prandtl (no slip) boundary condition holds for all wetted surfaces. Further discussion of boundary conditions is deferred until later sections.

The overall heat transfer for this configuration is characterized by the average Nusselt number computed over the left wall surface. The average Nusselt number is a function of several geometric parameters, including wall widths and lengths, channel widths and length, and inlet widths. The average Nusselt number also depends upon the working fluid Prandtl number (Pr), the Rayleigh number (Ra), and the thermal conductivity of the wall material (k_w) and working fluid (k_a). The present study investigates numerically the average Nusselt number dependencies by varying a number of the parameters discussed above.

The investigation was performed by using a proprietary finite element analysis program known as COSMOS/M, developed by the Structural Research and Analysis Corporation. COSMOS/M was designed for applications ranging from micro-computers to mainframe machines.

The FLOWSTAR module of COSMOS/M was used for solving the equation system noted earlier. FLOWSTAR is a finite element program capable of solving two and three dimensional laminar or turbulent fluid flow and thermal problems including flows coupled with solid region conduction. For non-isothermal flows the fluid is assumed incompressible within the constraints of the Boussinesq approximation. Newtonian and non-Newtonian fluids may be modelled for laminar flow.

The governing equations are discretized using the Galerkin method of weighted residuals. For two dimensional problems, a four node quadrilateral element is used. The interpolation functions are bilinear for both temperature and velocity. The pressure variable is eliminated using the penalty function method. Further information on COSMOS/M and FLOWSTAR is included in Appendix A.

This investigation used a Digital Corporation 486, 66 Mhz computer with 24 MByte of RAM as the primary computing resource. A virtual disk (RAM disk) arrangement was used which significantly reduced computation times, with most cases converging in 30 minutes or less.

Background

The study of natural convection flows in a thermosyphon configuration has been and continues to be an area of considerable interest. Many investigations have been carried out. Much of the earlier work is summarized by Japikse (1973). A more recent review specific to the closed and open loop configurations is given by Mertol and Greif (1985).

Previous studies have looked at a great variety of boundary conditions and geometries. Typically either isothermal or isoflux boundary conditions are applied. This decouples the flow problem from the conduction problem existing in the walls, and implicitly assumes thin walls with large thermal conductivity. Thus, there has been little evaluation of the conduction heat transfer effects of the bounding walls. Some natural convection studies in rather closely related geometries (enclosures and vertical channels) have examined the wall conduction effects. Examples are Burch et al. (1985) and Kaminski and Prakash (1986). These studies lend insight, but do not address the geometry of interest here.

The present work investigates multiple inlets along with wall conduction. The open loop thermosyphon may exchange fluid with one or more large external reservoirs across outlet and inlet openings. A literature review indicates that all the previous works in this area are limited to one inlet and

one outlet. Therefore, the effects of multiple inlets are still unknown. The geometry explored in this research, essentially combines a "L" type channel with a "U" type channel. To the best knowledge of the author no information is available in the open literature which studies this configuration. The following paragraphs summarize some previous works which have the "U" configuration in common.

Lapin (1969) used an approximate analysis and experiment to evaluate the heat transfer capabilities of a "U" type open loop thermosyphon. The author was concerned with cooling of gas turbine blades, which continues to be an important application. Lapin found significant advantages over previous methods. In this case the body force is acceleration due to angular rotation, with coriolis acceleration further complicating the flow.

Torrance (1979) modelled groundwater flow in aquifers as naturally occurring open loop thermosyphons which are heated geothermally from below. Using analytical and numerical techniques the author determined critical Rayleigh numbers for the onset of flow, and exit temperatures. Torrance and Chan (1981) pursued this subject further by numerically considering the open loop thermosyphon embedded in a heat conducting solid, heated from below. A fluid with Prandtl number 2.8, and fluid/solid thermal conductivity ratio of 0.133 was used. Heat transfer rates were determined.

Bau and Torrance (1981) studied experimentally and analytically the dynamic performance of the same configuration, but with symmetric and asymmetric heating of the inlet, outlet, and horizontal legs. They found transient flow oscillations. Under appropriate conditions the oscillations may amplify and eventually cause flow reversal. In all cases steady state flow eventually prevailed. The oscillations are explained by the phase lag between change in heating conditions and generation of the thermal buoyancy force.

Clarksean (1993) studied experimentally the heat transfer characteristics of an open loop thermosyphon used to cool vertical, cylindrical heat sources. The geometry investigated is similar to the three concentric cylinder geometry discussed previously with the outermost surface thermally insulated. The author found that for sufficiently high Rayleigh numbers heat transfer rates became independent of channel width. This is explained by development of boundary layer flows and the limited interaction between boundary layers on adjacent surfaces. Comparison to numerical results [Miyatake et al. (1973)] for a similar geometry showed general agreement. Miyatake et al. considered parallel vertical plates, one with a uniform heat flux and the other adiabatic, but made no allowance for thermal conductivity in the bounding walls.

There is a wealth of information concerning flows in vertical channels or between parallel plates beginning with

Elenbass (1942) who found correlations for the average Nusselt number in terms of the Rayleigh number and channel aspect ratio. Several pertinent studies involving wall conduction in vertical channels and enclosures since Elenbass are discussed below.

Zinnes (1970) studied numerically the wall conduction effects for laminar natural convection from a single vertical plate with arbitrary heating. The results were experimentally verified. He found significant coupling between the natural convection flow and plate conduction. The plate to fluid thermal conductivity ratio (k_w/k_a) greatly affects the degree of coupling.

Kaminski and Prakash (1979) studied the effects of wall conduction in a square enclosure. They restricted the investigation to one conducting wall with three zero thickness walls completing the enclosure. They investigated numerically the overall heat transfer effects as a function of several parameters: Grashof (Gr) and Prandtl ($Pr = 0.7$) numbers, wall thickness to height ratio (t/L), and wall to fluid thermal conductivity ratio (k_w/k_a). For constant Gr and Pr , they found the overall heat transfer was a function of the independent parameter $k_w L/k_a t$. For a constant value of $k_w L/k_a t$ the fluid/solid interface temperature distribution is independent of k_w/k_a and L/t separately. The enclosure fluid "sees" the same thermal driving force, and thus the overall heat transfer is correlated well with this parameter.

Kim and Viskanta (1985) presented numerical and experimental heat transfer results for a planar rectangular enclosure, but with four finite conducting walls. Isothermal boundary conditions were imposed on the external vertical wall surfaces, while the horizontal walls were adiabatic. The authors found that wall conduction reduces the temperature difference across the enclosure fluid, stabilizes the flow, and reduces overall heat transfer. The thermal conductivity ratio, and wall geometry (thickness and length) were important parameters.

Burch et al. (1985) conducted numerical studies of natural convection between two finite conducting vertical plates. The authors report that wall conduction has significant effects on the natural convection heat transfer in comparison to constant temperature walls. The effects are greater at high Grashof numbers, low thermal conductivity ratios, and high wall thickness to channel width ratios. The wall/fluid interface temperature and heat flux distributions are not uniform and are influenced by wall conduction more at higher Grashof numbers.

Mallinson (1987) also investigated numerically natural convection heat transfer in a rectangular enclosure with length (l) and width (w). Walls with finite conductivity and thickness (t) form the lengthwise sides. He used a new approach in modelling the wall-to-fluid interface by deriving a separate equation for the interface temperature. The author

indicates the conditions between the limiting cases of perfectly conducting and adiabatic walls exist when $0.1 \leq (w/t)/K \leq 100$. In this expression K is the wall-to-fluid thermal conductivity ratio, and (w/t) is the enclosure-to-wall width ratio.

Kim et al. (1990) investigated wall conduction effects on laminar natural convection between asymmetrically heated (uniform heat flux) vertical plates. Parameters of interest included: solid to fluid thermal conductivity ratio, wall to channel thickness ratios, and Grashof number. They found significant reduction (22%) in overall Nusselt number due to wall conduction. This occurs at low thermal conductivity ratios, large thickness ratios, and increases with Grashof number.

A recent numerical study investigates mixed convection in a cavity with conducting walls and a localized heat source [Papanicolaou and Jaluria (1993)]. With the assumption of adiabatic walls, the authors reported an error of 5.4% for the average Nusselt number computed over the heat source. This was for the case of relatively low thermal conductivity ratio of 0.8. Error increases as the thermal conductivity ratio increases.

All the above studies which address wall conduction used the thermal conductivity ratio ($K = k_w/k_a$) as an independent parameter to correlate heat transfer results. This parameter arises from the nondimensional form of the continuous heat

flux condition at the wall-to-fluid interface. Geometric parameters related to wall conduction are more problem specific, but clearly geometry plays an important role.

None of the works cited above addressed the questions raised here: effect of wall conduction and multiple inlets in an open loop thermosyphon configuration. Therefore, investigation of these questions may lead to more efficient thermal design of heat transfer equipment.

Other references in addition to those cited previously were invaluable in the progress of the present problem. The fundamentals of buoyancy induced flows are presented thoroughly in a text by Gebhart et al. (1988). Other natural convection references consulted include texts by Kays and Crawford (1980), and Bejan (1984). The textbook by Patankar (1980) is based on finite difference methods but offers insight in the methodology of numerical investigations.

On the subject of finite element analysis several textbooks were found useful. Huebner and Thornton (1982), Chung (1978), and Burnette (1988) were important in understanding FEM so that the method was properly applied to the present problem.

PROBLEM FORMULATION

Introduction

For the present study the natural convection flow of interest is assumed to be a steady state, two dimensional, laminar, and viscous flow of a constant property fluid. The fluid is Newtonian and incompressible. No heat generation exists in either the fluid or solid regions. The surroundings consist of an extensive, quiescent, isothermal reservoir at constant temperature T_∞ . Thermal radiative heat transport is also neglected.

The Boussinesq approximation is invoked. It consists of two primary simplifying assumptions. The fluid density is assumed constant except in its interaction with the body force (gravity), from which buoyancy forces arise. All other thermophysical properties are assumed constant, and are evaluated at a selected reference temperature and pressure.

With the assumptions above the governing equations and boundary conditions are expressed in terms of the primitive variables velocity, temperature, and pressure. These equations are then nondimensionalized to isolate relevant nondimensional parameters.

Governing Equations

For the present problem, the fluid flow and heat transfer are described by the conservation laws for mass (continuity),

momentum (Navier-Stokes), and energy. These laws are expressed below by equations (1), (2), and (3) respectively. Heat transfer in the solid regions of the problem domain is described by the energy equation (4). The compressibility work and viscous dissipation terms of the energy equation have been neglected. Note the Boussinesq approximation has not yet been included explicitly in the momentum equation (2).

$$\nabla \cdot \bar{u} = 0 \quad (1)$$

$$\rho (\bar{u} \cdot \nabla) \bar{u} = -\nabla p + \mu \nabla^2 \bar{u} + \rho \bar{g} \quad (2)$$

$$\rho C_p (\bar{u} \cdot \nabla T) = k_a \nabla^2 T \quad (3)$$

$$k_w \nabla^2 T = 0 \quad (4)$$

As noted earlier, the driving force behind natural convection flow is the variation in density due to temperature gradients. For the thermal buoyancy force term to appear explicitly in the momentum equation (2), the Boussinesq approximation is used. The following paragraphs detail how it is applied to this problem.

First, the pressure term in equation (2) is replaced with a modified pressure known as the motion pressure. Motion pressure is understood simply as the difference between the actual pressure (p) at any point in the fluid, and the hydrostatic pressure (p_h) that would exist at the same point in the absence of fluid flow. Motion pressure ($p_m = p - p_h$) is due to acceleration, viscous forces, and buoyancy forces.

Consider the following equations (5) and (6). The divergence of the hydrostatic pressure (5) is simply the body force per unit volume due to gravity ($-g_y$). The motion pressure (p_m) divergence is given in equation (6).

$$\nabla p_h = -g_y \rho_\infty \quad (5)$$

$$\nabla p_m = \nabla p - \nabla p_h = \nabla(p - p_h) \quad (6)$$

The pressure gradient and body force terms ($-\nabla p + \rho \vec{g}$) of the momentum equation (2) are rewritten using equations (5) and (6). In the present problem note that $\vec{g} = -g_y$.

$$-\nabla p - \rho g_y = -\rho g_y - \nabla p_h - \nabla(p - p_h) \quad (7)$$

$$-\nabla p - \rho g_y = -g_y (\rho - \rho_\infty) - \nabla p_m \quad (8)$$

Equation (8) above, is substituted into the momentum equation (2) with the result shown below.

$$\rho (\vec{u} \cdot \nabla) \vec{u} = -\nabla p_m + \mu \nabla^2 \vec{u} - g_y (\rho - \rho_\infty) \quad (9)$$

The final term in equation (9) is the buoyancy force per unit volume. It is represented by the density difference which next is rewritten in terms of temperature. The definition for β , the coefficient of volumetric expansion (equation 10), is used to make a simple linear approximation for the buoyancy force term. The final form of the buoyancy force term appears as in equation (11).

$$\beta = -\frac{1}{\rho} \left(\frac{\partial \rho}{\partial T} \right)_p \quad (10)$$

$$-g_y (\rho - \rho_\infty) \approx g_y \rho \beta (T - T_\infty) \quad (11)$$

Gebhart et al. (1988) supplies arguments to support the validity of the approximation in equation (11). The final form of the momentum equation is equation (12).

$$\rho (\bar{u} \cdot \nabla) \bar{u} = -\nabla p_m + \mu \nabla^2 \bar{u} + \rho g_y \beta (T - T_\infty) \quad (12)$$

One objective of this development is to show the correct inlet temperature boundary condition. When the local temperature (T) is equal to the temperature of the surroundings (T_∞) the buoyancy force is zero. Fluid enters from the isothermal surroundings at temperature T_∞ . Any other temperature specified at the inlet would introduce a false buoyancy. This holds true except for low Rayleigh numbers where conduction effects extend across the inlet boundary.

The buoyancy term in equation (12) accounts for variation in hydrostatic pressure since when integrated it will be a function of vertical position. How well the buoyancy force term and the constant property formulation models the actual physics depends largely on the reference state selected. Further discussion of the reference state will follow.

Boundary conditions specific to the present problem are presented on the following page. Refer to Figure 2 for dimensioning nomenclature. Figure 3 presents a graphical representation of the boundary conditions used.

$$u=v=0 \text{ for } \left[\begin{array}{l} x = h_1 \text{ and } 0 \leq y \leq l_1 \\ h_1 \leq x \leq (h_1 + b + h_2 + w_1 + l_2) \text{ and } y = 0 \\ (h_1 + b + h_2 + w_1) \leq x \leq (h_1 + b + h_2 + w_1 + l_2) \text{ and } y = w_2 \\ x = (h_1 + b + h_2 + w_1) \text{ and } w_2 \leq y \leq l_1 \\ x = (h_1 + b) \text{ and } b \leq y \leq l_1 \\ x = (h_1 + b + h_2) \text{ and } b \leq y \leq l_1 \\ (h_1 + b) \leq x \leq (h_1 + b + h_2) \text{ and } y = b \end{array} \right] \quad (13)$$

$$T = T_w \text{ for } x = 0 \text{ and } 0 \leq y \leq l_1 \quad (14)$$

$$\frac{\partial T}{\partial n} = 0 \text{ for } \left[\begin{array}{l} 0 \leq x \leq (h_1 + b + h_2 + w_1 + l_2) \text{ and } y = 0 \\ 0 \leq x \leq h_1 \text{ and } y = l_1 \\ (h_1 + b + h_2 + w_1) \leq x \leq (h_1 + b + h_2 + w_1 + l_2) \text{ and } y = w_2 \\ x = (h_1 + b + h_2 + w_1) \text{ and } w_2 \leq y \leq l_1 \\ (h_1 + b) \leq x \leq (h_1 + b + h_2) \text{ and } y = l_1 \end{array} \right] \quad (15)$$

$$\left[\begin{array}{l} u = 0 \\ \tau_{yy} = 0 \\ \frac{\partial T}{\partial y} = 0 \end{array} \right] \text{ for } h_1 \leq x \leq (h_1 + b) \text{ and } y = l_1 \quad (16)$$

$$\left[\begin{array}{l} u = 0 \\ \tau_{yy} = 0 \\ T = T_\infty \end{array} \right] \text{ for } (h_1 + b + h_2) \leq x \leq (h_1 + b + h_2 + w_1) \text{ and } y = l_1 \quad (17)$$

$$\left[\begin{array}{l} v = 0 \\ \tau_{xx} = 0 \\ T = T_\infty \end{array} \right] \text{ for } x = (h_1 + b + h_2 + w_1 + l_2) \text{ and } 0 \leq y = w_2 \quad (18)$$

